Journal of
Applied Crystallography
ISSN 0021-8898

Received 10 October 2001
Accepted 4 February 2002

Thermal expansion and atomic displacement parameters of cubic $KMgF_3$ perovskite determined by high-resolution neutron powder diffraction

I. G. Wood,[a]* K. S. Knight,[b,c] G. D. Price[a] and J. A. Stuart[d]

[a]Research School of Geological and Geophysical Sciences, University College London, Gower Street, London WC1E 6BT, UK, [b]ISIS Facility, Rutherford Appleton Laboratory, Chilton, Didcot, Oxon OX11 0QX, UK, [c]Department of Mineralogy, The Natural History Museum, Cromwell Road, London SW7 5BD, UK, and [d]Porvair Ceramics Ltd, Bergen Way, King's Lynn, Norfolk PE30 2JG, UK. Correspondence e-mail: ian.wood@ucl.ac.uk

The structure of $KMgF_3$ has been determined by high-resolution neutron powder diffraction at 4.2 K, room temperature and at 10 K intervals from 373 K to 1223 K. The material remains cubic at all temperatures. The average volumetric coefficient of thermal expansion in the range 373–1223 K was found to be 7.11 (3) $\times 10^{-5}$ K^{-1}. For temperatures between 4.2 and 1223 K, a second-order Grüneisen approximation to the zero-pressure equation of state, with the internal energy calculated *via* a Debye model, was found to fit well, with the following parameters: θ_D = 536 (9) K, V_o = 62.876 (6) Å^3, K_o' = 6.5 (1) and (V_oK_o/γ') = 3.40 (2) $\times 10^{-18}$ J, where θ_D is the Debye temperature, V_o is the volume at T = 0, K_o' is the first derivative with respect to pressure of the incompressibility (K_o) and γ' is a Grüneisen parameter. The atomic displacement parameters were found to increase smoothly with T and could be fitted using Debye models with θ_D in the range 305–581 K. At 1223 K, the displacement of the F ions was found to be much less anisotropic than that in $NaMgF_3$ at this temperature.

1. Introduction

The petrology of the Earth's lower mantle is thought to be dominated by (Mg,Fe)SiO_3 perovskite (Ringwood, 1962) and the physical properties of this mineral are, therefore, of great interest within the Earth sciences (Hemley & Cohen, 1992). However, because of the very high pressures and temperatures necessary to perform experiments at lower-mantle conditions, the behaviour of (Mg,Fe)SiO_3 is not easily investigated. Consequently, in an attempt to predict the physical properties of this material, experimental studies of structurally similar compounds (Poirier *et al.*, 1983) have been combined with computer simulations (see *e.g.* Wentzcovitch *et al.*, 1993, 1995; Vočadlo *et al.*, 1995; Oganov *et al.*, 2000, 2001). For this purpose, the fluoride perovskites, in particular neighborite, $NaMgF_3$ (Chao *et al.*, 1961), provide useful analogues. Neighborite is isoelectronic with $MgSiO_3$ and shows the same orthorhombic (*Pbnm*) distortion from the ideal cubic aristotype at room temperature. In contrast, $KMgF_3$ remains cubic at all temperatures.

The impetus for this study of $KMgF_3$ was threefold. Firstly, it was desirable to obtain accurate thermal expansion data and to make measurements of the atomic displacement parameters for comparison with the results of computer simulation; in framework structures such as perovskites, the apparent average bond distances and thermal displacement parameters are intimately linked (Street *et al.*, 1997). In $NaMgF_3$, the behaviour is complicated by the large-amplitude atomic vibrations and changes in symmetry associated with condensing soft modes; $KMgF_3$ therefore provides a simpler system on which to test new computational methodology. Secondly, $KMgF_3$ has been suggested recently (N. L. Ross & W. Crichton, personal communication) as a suitable pressure calibrant in X-ray diffraction experiments using diamond-anvil cells; accurate knowledge of its thermal expansion would enable its use at elevated pressure (P) and temperature (T). Finally, interest has been shown in $KMgF_3$ as a material for technological applications such as electro-optics (see *e.g.* Fukuda *et al.*, 2001) and radiation dosimetry (see *e.g.* Getkin *et al.*, 1998). The structures and phase transitions in the solid solution $Na_{1-x}K_xMgF_3$ have been investigated recently by Zhao (1998) and by Chakhmouradian *et al.* (2001), but the only detailed examination of $KMgF_3$ at non-ambient temperatures is that of Muradyan *et al.* (1984), who determined the atomic displacement parameters at 293 and 123 K.

2. Experimental details

The sample of $KMgF_3$ was prepared by a precipitation reaction of aqueous solutions of KHF_2 and saturated $MgCl_2$. The precipitate was washed repeatedly with 0.1 *M* acetic acid, water and ethanol/methanol; finally it was heated in a platinum crucible, with the sample surface covered with

platinum foil, at 973 K for 4 h in an N_2 atmosphere. An X-ray powder diffraction pattern of the resulting material showed that it also contained a small amount of MgF_2, the strongest peak from this being just less than 1% of the height of the strongest $KMgF_3$ reflections; no account was taken of this phase in the data analysis since there is little overlap between the strong reflections from MgF_2 and the peaks from $KMgF_3$.

The neutron powder diffraction data were collected using the high-resolution powder diffractometer (HRPD; Ibberson *et al.*, 1992) at the ISIS neutron spallation source of the Rutherford Appleton Laboratory (RAL). HRPD must be considered as an almost unrivalled instrument for lattice-parameter studies. In general, as a result of the high penetration and large physical size of the apparatus, neutron powder diffraction suffers far less from geometrical and physical aberrations than does X-ray diffraction. In addition, since the neutron time-of-flight technique offers effectively constant resolution across the entire range of d spacings, precise cell parameters may be obtained from strong low-index reflections, enabling rapid data collection. The normal disadvantage of neutron powder diffraction, namely low resolution, is overcome by the approximately 100 m flight path of the instrument. This allows a resolution in lattice spacings ($\Delta d/d$) of 5×10^{-4} to be achieved over the range $0.3 < d < 6.0$ Å, where Δd is the full width at half-height of the diffraction peak of spacing d. It should be noted, however, that profile refinement techniques allow shifts in peak positions to be determined to two orders of magnitude better than this (see below).

To confirm that the material remains cubic at all temperatures, a data set was collected at 4.2 K, counting for approximately 5 h. Further data were then collected at ambient temperature (counting for approximately 35 min) and in 10 K steps from 373 to 1223 K. During this sequence, approximately 2 min was allowed for thermal equilibration at each temperature, followed by measurement of the diffraction pattern for 13 min. Finally, to enable good values of the thermal parameters to be obtained, nine sets of data were collected at 1223 K, with a combined counting time of 26 h. In all cases the detectors used were in backscattering geometry, with $2\theta \simeq 168^\circ$. The patterns at and above ambient temperature were measured over the range of flight times from 20 to 120 ms ($0.41 < d < 2.49$ Å); the data at 4.2 K were collected using a slightly different range (30–130 ms; $0.62 < d < 2.69$ Å). The temperature stability was to within ± 0.1 K throughout.

The cell and thermal parameters were obtained by Rietveld refinement using the RAL's suite of programs based on the *Cambridge Crystallography Subroutine Library* (*CCSL*; Brown & Matthewman, 1993). The material has space group $Pm\bar{3}m$, with atomic fractional coordinates chosen as follows: K 1/2, 1/2, 1/2; Mg 0, 0, 0; F 1/2, 0, 0. Eighteen variables were included in the refinements (scale factor, cell parameter, four atomic displacement parameters, two half-width parameters, and ten coefficients for the Chebyschev polynomial function used to model the background). For the high-temperature data, a d-spacing range of $0.456 < d < 2.175$ Å was used in the refinements, with 5211 data points; values of χ^2 of typically $\sim$1.0 were obtained for the data sets with short collection times (indicating that the relatively poor counting statistics are unable to reveal any deficiencies in the model fitted). For the data sets collected for longer times at 1223 K, χ^2 was typically $\sim$1.7. A slightly different d-spacing range was used for the refinement of the data at 4.2 K ($0.663 < d < 2.527$ Å; 4462 data points) for which $\chi^2 = 7.94$.[1]

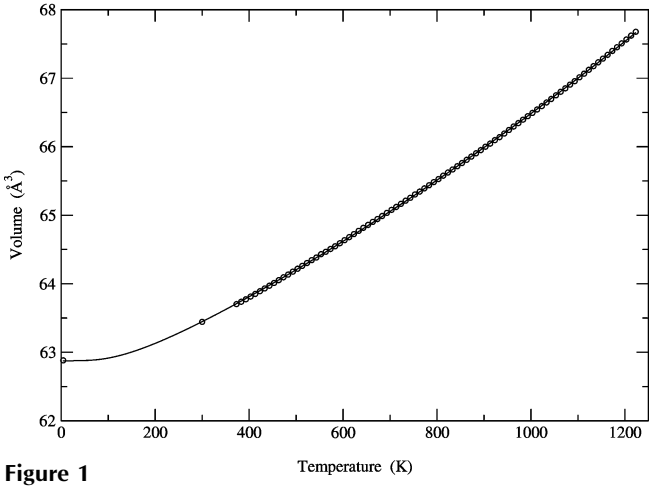

Figure 1
$KMgF_3$: unit-cell volume as a function of temperature. Open circles show measured data points. The full line shows the fit of the data to a second-order Grüneisen approximation to the zero-pressure equation of state (see text for details).

3. Results and discussion

3.1. Thermal expansion

Fig. 1 shows the variation of unit-cell volume with temperature over the complete temperature range covered in the experiments. For all data sets collected above room temperature, the standard uncertainties of the cell parameters obtained from the results of the Rietveld refinements were 0.00002 Å (for the 4.2 K data a value of 6×10^{-6} Å was obtained). This error leads to a corresponding constant error in cell volume of 0.001 Å^3, which appears to be consistent with the degree of scatter in the numerically differentiated thermal expansion curve (Fig. 2, see below).

To obtain thermal expansion values in the form tabulated by Fei (1995) the data above room temperature were fitted to

$$V(T) = V_{T_r} \exp\left[\int_{T_r}^{T} \alpha(T)\,\mathrm{d}T\right], \qquad (1)$$

where V_{T_r} is the volume at a chosen reference temperature, T_r, and $\alpha(T)$ is the thermal expansion coefficient, having the form

$$\alpha(T) = a_o + a_1 T. \qquad (2)$$

[1] The numbered intensity of each measured point on the profiles and the final output from the refinement program are available from the IUCr electronic archives (Reference: KS0117). Services for accessing these data are described at the back of the journal.

This fit gave values of V_{T_r} = 63.427 (2) Å^3, a_o = 5.08 (3) × 10^{-5} K^{-1} and a_1 = 2.54 (3) × 10^{-8} K^{-2}, for a chosen T_r of 300 K (it should be noted that when fitting the cell volumes and displacement parameters, the data point at 'room temperature' was always excluded, since its temperature was not sufficiently well known).

Alternatively, if it is assumed that the thermal expansion coefficient, α, in equation (1) is temperature independent, *i.e.* putting

$$\alpha(T) = \alpha_o, \tag{3}$$

we obtain α_o = 7.11 (3) × 10^{-5} K^{-1} and V_{T_r} = 63.27 (1) Å^3, again for T_r = 300 K.

A more physically meaningful interpretation of the thermal expansion curve can be obtained by using Grüneisen approximations for the zero-pressure equation of state (see Wallace, 1998), which allow estimates of the Debye temperature of the material to be made. For data covering a wide temperature range, the second-order Grüneisen approximation is more appropriate than the first-order approximation (Vočadlo *et al.*, 2002) and this takes the form

$$V(T) = V_o U/(Q - bU) + V_o, \tag{4}$$

where $Q = V_o K_o/\gamma'$ and $b = (K_o' - 1)/2$; γ' is a Grüneisen parameter (assumed constant), K_o and K_o' are the incompressibility and its first derivative with respect to pressure, respectively, at T = 0, and V_o is the volume at T = 0. The internal energy, U, may be calculated using the Debye approximation (see *e.g.* Cochran, 1973) from

$$U(T) = 9Nk_BT\left(\frac{T}{\theta_D}\right)^3 \int_0^{\theta_D/T} \frac{x^3\,\mathrm{d}x}{\exp(x) - 1}, \tag{5}$$

where N is the number of atoms in the unit cell, k_B is Boltzmann's constant and θ_D is the Debye temperature.

The solid line in Fig. 1 shows the result obtained from fitting the data to equation (4), with the resulting values of the four fitted constants: θ_D = 536 (9) K, Q = 3.40 (2) × 10^{-18} J, V_o = 62.876 (6) Å^3 and b = 2.73 (6). It can be seen that the fit to the data is excellent over the full temperature range of the experiment. This point is perhaps better illustrated in Fig. 2, which shows the behaviour of the thermal expansion coefficient, $\alpha(T)$, obtained from

$$\alpha(T) = (1/V)(\mathrm{d}V/\mathrm{d}T). \tag{6}$$

The full line in the figure gives the result obtained by differentiation of equation (4), while the points show the results from simple numerical differentiation by differences of the $V(T)$ data. In general, the two correspond very well, although there is perhaps a slight indication that the theory underestimates the expansion coefficient for temperatures above 1000 K, as anharmonicity becomes increasingly important.

An alternative, independent estimate of the Debye temperature may be obtained, assuming that all atoms play an equal mechanical role, from the average sound velocity and mean atomic mass of the material; Poirier (1991, equation 3.37 therein) gives

$$\theta_D = 2.512(\rho/\bar{M})^{1/3} v_m, \tag{7}$$

where ρ is the density, $\bar{M}$ is the mean atomic mass (kg mol^{-1}) and v_m is the average sound velocity. For $KMgF_3$, at room temperature, ρ = 3.151 × 10^3 kg m^{-3}, $\bar{M}$ = 24.08 × 10^{-3} kg mol^{-1} and v_m = 4.29 km s^{-1} [value for v_m taken from Table 5.4 of Poirier (1991); note, however, that the listed Debye temperatures in this table are all in error by a factor of $5^{1/3}$]. These values give θ_D = 547 K, in excellent agreement with the result obtained from the analysis of the thermal expansion curve.

Although equation (4) provides a useful framework within which to assess the behaviour of the material, it should be pointed out that the theory suffers from a number of deficiencies. Firstly, a harmonic approximation is used to calculate $U(T)$; this will, in general, become less exact as the temperature increases and anharmonicity becomes of greater importance. Secondly, recent calculations for $MgSiO_3$ by Oganov *et al.* (2000) have indicated that in some respects the Debye approximation works rather poorly for perovskites; it was found that although the Debye model reproduced the heat capacity curve above 500 K quite accurately, it gave thermal expansion and Grüneisen parameter values that were too small. In addition, projections of the calculated vibrational density of states on to each of the atomic species showed that contributions from different atoms were localized in different parts of the spectrum, with, as might be expected, the A-cation contribution occurring at lower frequencies than that from the B cation.

These deficiencies in the model will be reflected in the fitted values of the four parameters, which should, therefore, be treated with some caution. An estimate of the pressure derivative of the incompressibility, K_o', may be obtained from the coefficient b. The result obtained in this way from the present study, K_o' = 6.5 (1), is in fair agreement with that from single-crystal high-pressure X-ray diffraction studies using a diamond-anvil pressure cell [K_o' = 5.1 (2); W. Crichton, N.

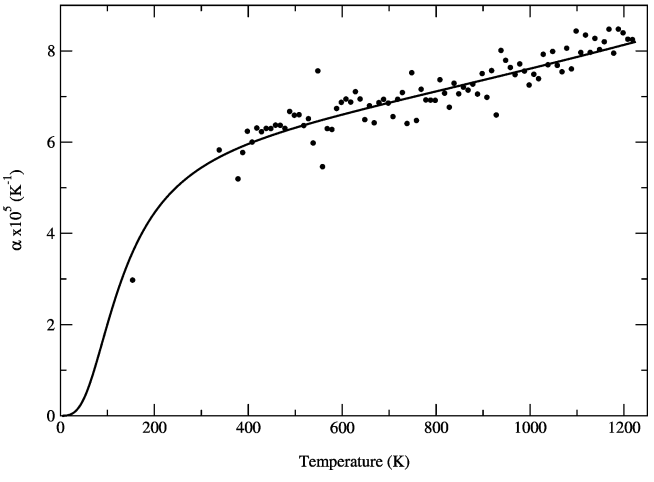

Figure 2
$KMgF_3$: volumetric thermal expansion coefficient as a function of temperature. The points were obtained by numerical differentiation of the data shown in Fig. 1; the solid line was obtained *via* equation (4).

Ross, personal communication]. Determination of the incompressibility, K_o, from the coefficient Q in equation (4) is possible only if the value of the Grüneisen parameter, γ', is known. Using the value of K_o [73.0 (4) GPa] from this X-ray diffraction experiment allows us to obtain the result γ' = 1.35 (1). The thermodynamic Grüneisen parameter, $\gamma_{\rm th}$, may be defined (see *e.g.* Poirier, 1991) as

$$\gamma_{\rm th} = \alpha K_T V/C_v, \tag{8}$$

where K_T is the isothermal incompressibility and C_v is the specific heat at constant volume. Differentiating equation (4) and recalling that $C_v = {\rm d}U/{\rm d}T$, gives us the following expression for $\gamma_{\rm th}$ within the second-order Grüneisen approximation:

$$\gamma_{\rm th} = [QV_o/(Q - bU)^2]K_T. \tag{9}$$

Using the value of K_o of Crichton & Ross (personal communication), equation (9) gives $\gamma_{\rm th}$ = 1.42 at 300 K; this agrees well with the range of values reported for perovskites (see *e.g.* Anderson, 1989; Poirier, 1991; Oganov *et al.*, 2000, 2001) but is a little lower than that previously quoted for $KMgF_3$ itself (1.60; Anderson, 1989).

3.2. Atomic displacement parameters

The behaviour of the displacement parameters ($\overline{u_{ij}^2}$) as a function of temperature is presented in Fig. 3. The displacements of the K and Mg ions are constrained by symmetry to be isotropic, whereas the locus of the F ions is a flattened disk elongated at right angles to the axis of the average Mg—F bond (*i.e.* perpendicular to the edge of the unit cell on which the F ion lies). The values shown between 373 and 1223 K were all obtained from the data sets collected with short counting times used to determine the cell parameters; for clarity, in this diagram only the high-temperature data are presented and error bars are shown only at selected temperatures. At 4.2 K, the displacement parameters were found to be: K, 0.0007 (2); Mg, 0.0005 (2); F($\overline{u_{11}^2}$), 0.0003 (3); F($\overline{u_{33}^2}$), 0.0027 (2) Å^2. At room temperature, the values are similar to those obtained by Muradyan *et al.* (1984) at 298 K [K, 0.0108; Mg, 0.0059; F($\overline{u_{11}^2}$), 0.0066; F($\overline{u_{33}^2}$), 0.0144 Å^2]. At 1223 K, the values obtained from the mean of seven data sets (each counted for approximately 25 min) were: K, 0.0446 (2); Mg, 0.0212 (1); F($\overline{u_{11}^2}$), 0.0208 (2); F($\overline{u_{33}^2}$), 0.0481 (1) Å^2.

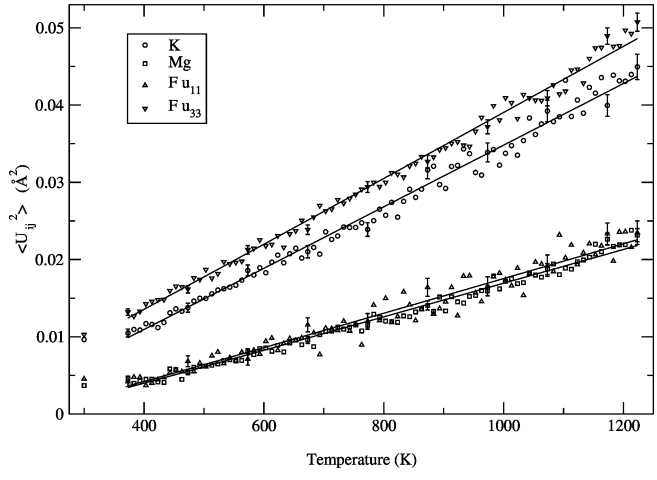

Figure 3
$KMgF_3$: atomic displacement parameters as a function of temperature. For clarity, error bars are shown only at selected temperatures. The full lines were obtained *via* equation (7) (for details see text).

It is apparent from Fig. 3 and from the data listed above that the displacement parameter of the Mg ion is identical in value to F($\overline{u_{11}^2}$) at all temperatures. Since only the Bragg reflections have been measured, it is formally invalid to draw any conclusions about pair correlation of the atomic motions; nevertheless, this result is highly suggestive that the vibrations of the two atoms along the line of the Mg—F bond are highly coupled and that the thermal motion of the MgF_6 octahedra may be considered in terms of rotations and translations of a quasi-rigid unit. It is perhaps slightly surprising to note that at high temperatures the motion of the F ions becomes less anisotropic as the temperature increases; for example, at 373 K, F($\overline{u_{33}^2}$) $\simeq$ 3F($\overline{u_{11}^2}$), whereas at 1223 K, F($\overline{u_{33}^2}$) $\simeq$ 2F($\overline{u_{11}^2}$). The degree of anisotropy shown by $KMgF_3$ is considerably less than that found in the cubic phase of $NaMgF_3$, for which Street *et al.* (1997) determined the following displacement parameters at 1223 K: Na, 0.0951 (3); Mg, 0.0279 (2); F($\overline{u_{11}^2}$), 0.0266 (3); F($\overline{u_{33}^2}$), 0.1283 (2) Å^2. For $NaMgF_3$, F($\overline{u_{33}^2}$) $\simeq$ 5F($\overline{u_{11}^2}$), reflecting the much greater softness of the optic rotational modes of the coupled MgF_6 octahedra, which persists even at a temperature 183 K above the transition to cubic symmetry. Both Fourier maps and molecular-dynamics simulations of $NaMgF_3$ (Street *et al.*, 1997) showed that the maximum in the probability density of the F atoms occurred at the midpoint of the Mg–Mg line and there is, therefore, no reason to suppose that the distribution resembles a torus rather than a discus. Although we have not carried out a similar analysis for $KMgF_3$, we would expect to obtain this result also for this material, for which the anisotropy of the thermal motion is less extreme. The effect of rotational optic modes in cubic perovskites is to produce a volumetric 'dynamic lattice contraction', estimated from molecular-dynamics simulations to be as large as 4–6% in the case of $NaMgF_3$ (Street *et al.*, 1997). Clearly, in $KMgF_3$ the smaller anisotropy will result in a cubic cell parameter that is more nearly equal to twice the equilibrium Mg—F bond distance. The magnitude of the displacement parameter of the A cation in its 12-fold coordinated cubo-octahedral site provides a further interesting contrast between the two materials; at 1223 K, $\overline{u^2}$ for K is approximately half $\overline{u^2}$ for Na, reflecting the greater tendency of the smaller lighter Na ion to 'rattle' in the central cage.

Following Lonsdale (1962), we may describe the variation of thermal displacement parameter with temperature according to a Debye model as

$$\overline{u^2} = (145.55T/M\theta_D^2)\varphi(\theta_D/T) + A, \tag{10}$$

where M is the mass of the vibrating species in atomic mass units and the function $\varphi(\theta_D/T)$ is given by

$$\varphi\left(\frac{\theta_D}{T}\right) = \frac{T}{\theta_D}\int_0^{\theta_D/T}\left[\frac{x}{\exp(x)-1}\right]\mathrm{d}x. \qquad (11)$$

In principle, the constant, A, which is directly related to the zero-point energy of the atoms, is fixed for given values of M and θ_D, being given by $A = 36.39/M\theta_D$. This reduces equation (10) to a single-parameter fit but requires that the absolute magnitude of the displacement parameters is accurately known. In practice, a much better fit to the observed data is generally obtained by including A as a second refineable parameter, thereby modelling the change in $\overline{u^2}$ with temperature but allowing for a constant offset from uncorrected systematic errors. The lines shown in Fig. 3 were obtained in this way by fitting equation (10) to the data (including also the 4.2 K data points). The fit at high temperatures is clearly very good, but it should be noted that extrapolation to 4.2 K gives rather poor agreement with the measured values. The following Debye temperatures were obtained from the four sets of atomic displacement parameters: K, 305 (2); Mg, 522 (4); F($\overline{u_{11}^2}$), 581 (7); F($\overline{u_{33}^2}$), 422 (2) K; these may, in turn, be expressed as characteristic vibrational frequencies with values 6.36 (4) $\times 10^{12}$, 10.88 (8) $\times 10^{12}$, 12.1 (2) $\times 10^{12}$ and 8.79 (4) $\times 10^{12}$ Hz, respectively. The lower Debye temperatures and characteristic frequencies for K and F($\overline{u_{33}^2}$) reflect the relative greater softness of the A-cation displacements and rotational optic modes of the octahedra compared with the B-cation and vibrational octahedral displacements. Similar features were observed by Oganov *et al.* (2000) in their projected vibrational density of states. In contrast, the mean value of the Debye temperatures from Mg and F($\overline{u_{11}^2}$), 552 (8) K, agrees well with that obtained from analysis of the thermal expansion curve [536 (9) K], suggesting that increase of the Mg—F bond length has a more dominant role in determining the value of the thermal expansion coefficient in $KMgF_3$ than is the case for $NaMgF_3$, in which the rotational modes of the octahedra also make a significant contribution (Street *et al.*, 1997).

We would like to thank Dr L. Vočadlo for assistance with the analysis of the data and Dr W. Crichton for kindly providing us with values of K_o and K_o'.

References

Anderson, D. L. (1989). *Theory of the Earth*. Oxford: Blackwell.

Brown, J. & Matthewman, J. C. (1993). Report RAL-93-009, Rutherford Appleton Laboratory, Oxford.

Chakhmouradian, A. R., Ross, K. D., Mitchell, R. H. & Swainson, I. (2001). *Phys. Chem. Miner.* **28**, 277–284.

Chao, E. C. T., Evans, H. T., Skinner, B. J. & Milton, C. (1961). *Am. Miner.* **46**, 379–393.

Cochran, W. (1973). *The Dynamics of Atoms in Crystals*. London: Arnold.

Fei, Y. (1995). *AGU Reference Shelf 2: Mineral Physics and Crystallography – A Handbook of Physical Constants*, edited by T. J. Ahrens, pp. 29–44. Washington: AGU.

Fukuda, T., Shimamura, K., Yoshikawa, A. & Villora E. G. (2001). *Opto-electron. Rev.* **9**, 109–116.

Getkin, A. V., Krasovitskaya, I. M. & Shiran, N. V. (1998). *Radiat. Meas.* **29**, 337–340.

Hemley, R. J. & Cohen, R. E. (1992) *Annu. Rev. Earth Planet. Sci.* **20**, 553–600.

Ibberson, R. M., David, W. I. F. & Knight, K. S. (1992) Report RAL-92-031, Rutherford Appleton Laboratory, Oxford.

Lonsdale, K. (1962). *Temperature and Other Modifying Factors*, in *International Tables for X-ray Crystallography*, Vol. III, edited by C. H. MacGillavry & G. D. Riek. Birmingham: Kynoch Press.

Muradyan, L. A., Zavodnik, V. E., Makarova, I. P., Aleksandrov, K. S. & Simonov, V. I. (1984). *Kristallografiya*, **29**, 392–394.

Poirier, J. P. (1991). *Introduction to the Physics of the Earth's Interior*. Cambridge University Press.

Poirier, J. P., Peyronneau, J., Gesland, J. Y. & Brébec, G. (1983). *Phys. Earth Planet. Inter.* **32**, 273–287.

Oganov, A. R., Brodholt, J. P. & Price, G. D. (2000). *Phys. Earth Planet. Inter.* **122**, 277–288.

Oganov, A. R., Brodholt, J. P. & Price, G. D. (2001). *Earth Planet Sci. Lett.* **184**, 555–560.

Ringwood, A. E. (1962). *J. Geophys. Res.* **67**, 4005–4010.

Street, J. N., Wood, I. G., Knight, K. S. & Price, G. D. (1997). *J. Phys. Condens. Matter*, **9**, L647–L655.

Vočadlo, L., Patel, A. & Price, G. D. (1995). *Miner. Mag.* **59**, 597–605.

Vočadlo, L., Knight, K. S., Price, G. D. & Wood, I. G. (2002). *Phys. Chem. Miner.* In the press.

Wallace, D. C. (1998). *Thermodynamics of Crystals.* New York: Dover.

Wentzcovitch, R. M., Martins, J. L. & Price, G. D. (1993). *Phys. Rev. Lett.* **70**, 3947–3950.

Wentzcovitch, R. M., Ross, N. L. & Price, G. D. (1995). *Phys. Earth Planet. Inter.* **90**, 101–112.

Zhao, Y. (1998) *J. Solid State Chem.* **141**, 121–132.